

## COMPARATIVE STUDY REGARDING THE FORMATION OF $\text{La}_{1-x}\text{Sr}_x\text{CrO}_3$ PEROVSKITE USING UNCONVENTIONAL SYNTHESIS METHODS

R. Ianoș<sup>1\*</sup>, C. Păcurariu<sup>1</sup>, I. Lazău<sup>1</sup>, S. Ianoșev<sup>1</sup>, Z. Ecsedi<sup>1</sup>, R. Lazău<sup>1</sup> and P. Barvinschi<sup>2</sup>

<sup>1</sup>‘Politehnica’ University of Timișoara, Faculty of Industrial Chemistry and Environmental Engineering, P-ța Victoriei No. 2  
Timișoara 300006, Romania

<sup>2</sup>The West University of Timișoara, Faculty of Physics, V. Pârvan No. 4, Timișoara, Romania

The synthesis of strontium-doped lanthanum chromite,  $\text{La}_{1-x}\text{Sr}_x\text{CrO}_3$  ( $x=0.1$  and  $0.3$ ), used as an interconnect material for solid oxide fuel cells (SOFC), was investigated using two unconventional synthesis methods: (1) organic precursors' method based on the thermal conversion of complex combination resulted in the oxidation reaction of 1,2-ethanediol by  $\text{La}^{3+}$ ,  $\text{Sr}^{2+}$  and  $\text{Cr}^{3+}$  nitrates; (2) combustion synthesis based on the exothermic redox reaction of  $\text{La}^{3+}$ ,  $\text{Sr}^{2+}$  and  $\text{Cr}^{3+}$  nitrates with urea and glycine as fuels. We also used a mixture of urea and glycine as fuel. The samples were characterized by means of thermal analysis and X-ray diffraction.

**Keywords:** combustion synthesis, fuel cells, interconnect material, organic precursors, perovskite

### Introduction

Solid oxide fuel cells (SOFCs) offer a new technology that directly converts chemical into electrical energy and represent a promising alternative over the traditional energy conversion systems. Besides the high efficiency and fuel adaptability, SOFCs provide many other advantages including reliability, modularity, and almost entirely nonpolluting technology, practically without  $\text{NO}_x$  and  $\text{SO}_x$  emissions [1].

By using only solid materials, including the electrolyte, the SOFCs are more compact and can be more easily manipulated, and thus, multiple cells can be stacked in series to increase the energy efficiency. In order to do this, each individual cell is electrically connected to another cell using an interconnect material. The role of the interconnect material is to provide the electrical connection between adjacent cells and to keep fuel and oxidant apart.

The high operating temperature of the SOFC, approximately 1000°C, imposes severe conditions for the component materials of the cells. Because the interconnect is exposed simultaneously to the reducing environment of the anode and to the oxidizing atmosphere of the cathode, the potential interconnect materials must meet the most stringent requirements of all the cell components: excellent electrical conductivity, thermal expansion coefficient comparable to those of the other cell components, lack of porosity in order to avoid mixing of fuel and oxygen, good mechanical strength as well as chemical and physical stability [2].

Although the metallic interconnects are more cost effective, they are prone to oxidation and cannot be used at high temperatures. Thus, ceramic materials represent a successful choice as interconnect materials. Lanthanum chromite-based materials,  $\text{LaCrO}_3$ , which belong to the perovskite family, are the most promising interconnect materials for SOFCs. The properties of lanthanum chromite can be significantly improved by substituting either  $\text{La}^{3+}$  or  $\text{Cr}^{3+}$  in the perovskite structure with different metal cations (e.g.,  $\text{Ca}^{2+}$ ,  $\text{Sr}^{2+}$ ,  $\text{Ni}^{2+}$ ,  $\text{Mg}^{2+}$ ,  $\text{Cu}^{2+}$ , etc.) as well as by optimizing the chemical stoichiometry of dopant cations. The poor sintering behavior of these materials can be improved by using highly reactive powders with high surface area [3–5].

Several methods for the low-temperature synthesis of doped  $\text{LaCrO}_3$  have been developed in order to achieve the desired properties of powders: co-precipitation route [6], sol-gel [7], organic precursors [8, 9], hydrothermal synthesis [10, 11], Pechini [12] and microwave heating technique [13]. One of the most promising and frequently used techniques is the combustion synthesis using urea [14, 15], glycine [16–20], or citric acid [21, 22] as fuels. Concerning the preparation of complex metal oxide nanocrystalline powders at low temperatures, previous studies [23, 24] have shown a number of advantages exhibited by the organic precursors' method as well as by combustion synthesis [24–26].

From this point of view, the aim of this paper is to investigate the strontium-doped lanthanum chromite,  $\text{La}_{1-x}\text{Sr}_x\text{CrO}_3$  ( $x=0.1$  and  $0.3$ ), powder prepara-

\* Author for correspondence: robert\_ianos@yahoo.com

tion using two unconventional synthesis methods: organic precursors' method and combustion synthesis.

## Experimental

### Materials

The starting raw materials were all pro analysis purity degree:  $\text{La}(\text{NO}_3)_3 \cdot 6\text{H}_2\text{O}$  (Merck),  $\text{Cr}(\text{NO}_3)_3 \cdot 9\text{H}_2\text{O}$  (Merck),  $\text{Sr}(\text{NO}_3)_2$  (Merck), 1,2-ethanediol (Fluka), urea (Merck), glycine (Merck).

### Organic precursors' method

The method is based on thermal conversion of the complex combinations resulting in the oxidation of 1,2-ethanediol,  $\text{C}_2\text{H}_6\text{O}_2$ , to the glyoxilate dianion,  $\text{C}_2\text{H}_2\text{O}_4^{2-}$ , by  $\text{La}^{3+}$ ,  $\text{Sr}^{2+}$  and  $\text{Cr}^{3+}$  nitrates. The aqueous solution of  $\text{La}^{3+}$ ,  $\text{Sr}^{2+}$  and  $\text{Cr}^{3+}$  nitrates and 1,2-ethanediol, with an excess of 25% of 1,2-ethanediol was heated in air up to 100°C. During the exothermic reaction, the  $\text{NO}_x$  gases were eliminated, resulting the complex combination as a green-black powder, which was subsequently washed out with acetone–water mixture and then filtered.

### Combustion synthesis

In the first stage, the individual reactivity of each metal nitrate with respect to urea ( $\text{CH}_4\text{N}_2\text{O}$ ) and glycine ( $\text{C}_2\text{H}_5\text{NO}_2$ ) was tested (Table 1). In the second stage, the desired solid solutions ( $\text{La}_{0.9}\text{Sr}_{0.1}\text{CrO}_3$ ,  $\text{La}_{0.7}\text{Sr}_{0.3}\text{CrO}_3$ ) were synthesized using the following fuels: urea (U), glycine (G), and a mixture of urea and glycine (UG). All samples were designed assuming that  $\text{CO}_{2(g)}$ ,  $\text{H}_2\text{O}_{(g)}$  and  $\text{N}_{2(g)}$  are the resulting by-products of the combustion reaction. Stoichiometric metal nitrate–fuel molar ratios were used. After dissolving the desired metal nitrates in the right proportion in a minimum volume of distilled water, the required amount of fuel was added: urea, glycine and a mixture of urea and glycine. The resulting solution was then heated up to 300°C in order to promote water evaporation and the initiation of the combustion

reaction. During the heating process ignition occurred, followed by the combustion of the reactants' mixture, with the appearance of a high speed propagating flame. The high temperature reached within the raw material mixture led to the formation of dried fluffy foam, which could be easily crumbled into a fine powder.

### Instrumental methods

The as-prepared powders were annealed in an electric furnace at temperatures ranging between 1000 and 1350°C with one-hour soaking time. The thermal behavior of the samples was monitored using a TG/DTA Diamond Perkin Elmer derivatograph. The data were recorded in static air atmosphere, using Pt crucible and a heating rate of 10°C min<sup>-1</sup>.

The evolution of the phase composition of the samples was monitored by XRD using a Bruker's D8 Advanced system,  $\text{CuK}_\alpha$  radiation. The average crystallite size was determined based on the XRD patterns –  $h k l$  planes 1 1 2 and 0 0 4 – using Scherrer's equation:

$$D = \frac{0.9\lambda}{\beta \cos \theta} \quad (1)$$

where  $D$  is the crystallite size in nm,  $\lambda$  is radiation wavelength ( $\text{CuK}_\alpha$ , 0.15406 nm),  $\beta$  is the full width at half of maximum in radians, and  $\theta$  is the Bragg-angle.

## Results and discussion

The main characteristics of the combustion reaction of each metal nitrate with urea and glycine are presented in Table 1.

As can be seen in Table 1, there is a different behaviors of each metal nitrate with respect to urea and glycine. From this point of view, the similar behavior of lanthanum and strontium nitrate with respect to the two fuels needs to be emphasized. In both cases, glycine proves to be the only fuel that reacts with these metal nitrates, leading to the development of an explosion type combustion reaction. On the other hand,

**Table 1** Characteristics of the combustion reaction of metal nitrates with urea and glycine

Metal nitrate	Theoretical amount of oxide/mol	Fuel	Reaction time/s	Experimental observations <sup>a</sup>	Phase composition of the resulting powders
$\text{La}(\text{NO}_3)_3 \cdot 6\text{H}_2\text{O}$	0.02	urea glycine	— 0	NH <sub>3</sub> , white, no combustion white, flame explosion	$\text{LaONO}_3$ $\text{La}_2\text{O}_3$
$\text{Cr}(\text{NO}_3)_3 \cdot 9\text{H}_2\text{O}$	0.04	urea glycine	15 55	NH <sub>3</sub> , green, incandescence green, smoldering combustion	$\alpha\text{-Cr}_2\text{O}_3$ $\alpha\text{-Cr}_2\text{O}_3$
$\text{Sr}(\text{NO}_3)_2$	0.06	urea glycine	— 0	NH <sub>3</sub> , white, no combustion white, flame explosion	$\text{Sr}(\text{NO}_3)_2$ $\text{SrCO}_3$

<sup>a</sup>Observed gases, color of the resulting powder and combustion reaction type

chromium nitrate reacts with both urea and glycine, ensuring the formation of single-phase  $\alpha\text{-Cr}_2\text{O}_3$ .

Considering the velocity of the combustion reaction, one could notice that urea reacts faster with chromium nitrate than glycine. Based on these experimental observations, in general, and on the reaction time in particular, the different reactivities of lanthanum, strontium and chromium nitrates with respect to urea and glycine are pointed out. Considering the combustion reaction velocity as a criterion for the compatibility of metal nitrate/fuel mixtures, it is pointed out that glycine is the most suitable fuel for lanthanum and strontium nitrates, while urea seems to be the most adequate fuel for chromium nitrate.

The  $\text{La}_{0.7}\text{Sr}_{0.3}\text{CrO}_3$  synthesis reactions using urea, glycine and the mixture of urea and glycine can be represented by Eqs (2)–(4).

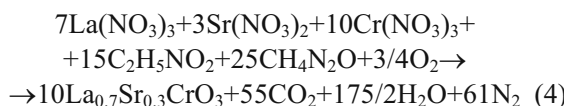
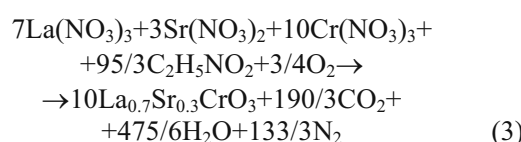
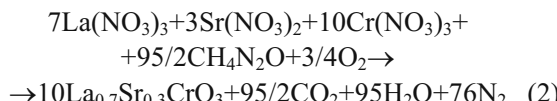
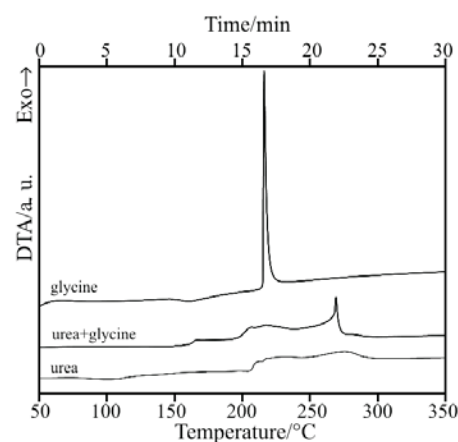


Figure 1 shows the DTA curves obtained for the mixture of lanthanum, chromium and strontium nitrates – dosed in the stoichiometric ratio corresponding to  $\text{La}_{0.9}\text{Sr}_{0.1}\text{CrO}_3$  – with urea, glycine and the mixture of urea and glycine, respectively.

As can be seen from Fig. 1, the heating behavior of the precursor mixtures containing the desired metal nitrates and various fuels is quite different. The use of glycine as a reducing agent alongside the corresponding metal nitrates (sample 6G) leads to the development of a very fast (5 s) and vigorous combustion re-



**Fig. 1** DTA curves of the raw material mixtures designed for the  $\text{La}_{0.9}\text{Sr}_{0.1}\text{CrO}_3$  combustion synthesis (samples 4U, 5UG and 6G)

action, evidenced by the presence of a strong and sharp exothermic effect at 216°C on the DTA curve.

Unlike glycine, urea (sample 4U) does not promote the evolution of a fast and intense combustion reaction. The broad weak exothermic effect, located between 210 and 290°C, is in excellent consistency with the development of the redox reaction, which lasts considerably longer (45 s). The precursor mixture containing both urea and glycine (sample 5UG) exhibits an intermediate behavior: the combustion reaction is significantly faster (10 s) and more exothermic than the sample with urea, but slower and less exothermic than the sample with glycine.

These results emphasize once again that there is a predilection of metal nitrates with respect to certain fuels. At the same time, the importance of selecting the right fuel is pointed out in order to achieve the maximum exothermic effect of the combustion reaction.

Regarding the phase formation succession for  $\text{La}_{0.7}\text{Sr}_{0.3}\text{CrO}_3$ , lanthanum chromate ( $\text{La}_2\text{CrO}_6$ ) and strontium chromate ( $\text{SrCrO}_4$ ) are mentioned first in the literature [27]. However, in the case of samples obtained directly from the combustion reaction, the

**Table 2** Crystalline phases identified on the XRD patterns

Sample	Designed stoichiometry	Synthesis method	Crystalline phases present on the XRD patterns			
			as-resulted	1000°C/1 h	1200°C/1 h	1350°C/1 h
1U			$\text{La}_{0.7}\text{Sr}_{0.3}\text{CrO}_3$ , $\text{Cr}_{1.01}\text{LaO}_{3\pm\delta}$	$\text{La}_{0.7}\text{Sr}_{0.3}\text{CrO}_3$ , $\text{SrCrO}_4$	$\text{La}_{0.7}\text{Sr}_{0.3}\text{CrO}_3$ , $\text{SrCrO}_4$	$\text{La}_{0.7}\text{Sr}_{0.3}\text{CrO}_3$ , $\text{SrCrO}_4$ (traces)
2UG	$\text{La}_{0.7}\text{Sr}_{0.3}\text{CrO}_3$	Combustion synthesis	$\text{La}_{0.7}\text{Sr}_{0.3}\text{CrO}_3$ , $\text{Cr}_{1.01}\text{LaO}_{3\pm\delta}$	$\text{La}_{0.7}\text{Sr}_{0.3}\text{CrO}_3$ , $\text{SrCrO}_4$	$\text{La}_{0.7}\text{Sr}_{0.3}\text{CrO}_3$ , $\text{SrCrO}_4$	$\text{La}_{0.7}\text{Sr}_{0.3}\text{CrO}_3$ , $\text{SrCrO}_4$ (traces)
3G			$\text{La}_{0.7}\text{Sr}_{0.3}\text{CrO}_3$ , $\text{Cr}_{1.01}\text{LaO}_{3\pm\delta}$	$\text{La}_{0.7}\text{Sr}_{0.3}\text{CrO}_3$ , $\text{SrCrO}_4$	$\text{La}_{0.7}\text{Sr}_{0.3}\text{CrO}_3$ , $\text{SrCrO}_4$	$\text{La}_{0.7}\text{Sr}_{0.3}\text{CrO}_3$ , $\text{SrCrO}_4$ (traces)
5UG	$\text{La}_{0.9}\text{Sr}_{0.1}\text{CrO}_3$		$\text{La}_{0.9}\text{Sr}_{0.1}\text{CrO}_3$	$\text{La}_{0.9}\text{Sr}_{0.1}\text{CrO}_3$	$\text{La}_{0.9}\text{Sr}_{0.1}\text{CrO}_3$	$\text{La}_{0.9}\text{Sr}_{0.1}\text{CrO}_3$
7	$\text{La}_{0.7}\text{Sr}_{0.3}\text{CrO}_3$	Organic precursors	amorphous	$\text{La}_{0.7}\text{Sr}_{0.3}\text{CrO}_3$ , $\text{SrCrO}_4$	$\text{La}_{0.7}\text{Sr}_{0.3}\text{CrO}_3$ , $\text{SrCrO}_4$	$\text{La}_{0.7}\text{Sr}_{0.3}\text{CrO}_3$ , $\text{SrCrO}_4$ (traces)
8	$\text{La}_{0.9}\text{Sr}_{0.1}\text{CrO}_3$		amorphous	$\text{La}_{0.9}\text{Sr}_{0.1}\text{CrO}_3$	$\text{La}_{0.9}\text{Sr}_{0.1}\text{CrO}_3$	$\text{La}_{0.9}\text{Sr}_{0.1}\text{CrO}_3$

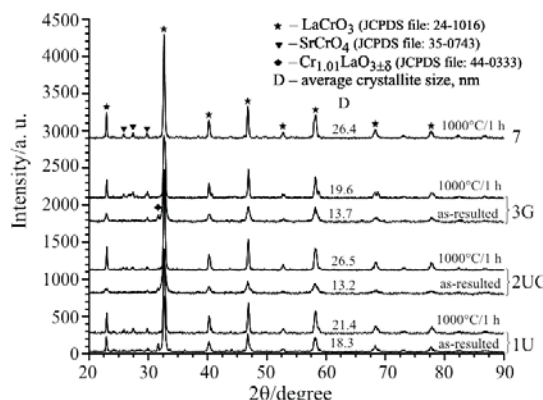


**Fig. 2** XRD patterns of the  $\text{La}_{0.7}\text{Sr}_{0.3}\text{CrO}_3$  prepared via combustion synthesis (using various fuels) and organic precursors

main crystalline phase is the  $\text{Sr}^{2+}$ -doped  $\text{LaCrO}_3$ , lacking the peaks of  $\text{SrCrO}_4$  (Table 2).

After annealing at  $1000^\circ\text{C}$ , some weak reflections of  $\text{SrCrO}_4$  occur, suggesting that during the combustion reaction a fraction of the  $\text{Sr}^{2+}$  content was bonded as amorphous  $\text{SrCrO}_4$ , which crystallized when heated (Fig. 2). This finding was also sustained by the yellow color of the samples' washing water, denoting the presence of soluble  $\text{Cr}^{6+}$ .

The peak from  $31.7^\circ$ , present in all samples resulting directly from the combustion synthesis (Fig. 2) can be attributed to a preceding phase of the projected strontium-doped lanthanum chromite in which the chromium oxidation state is intermediate between  $3+$  and  $6+$ . The composition attributed to this phase by the JCPDS file 44-0333 is  $\text{Cr}_{1.01}\text{LaO}_{3\pm\delta}$ .

In the case of using the combustion synthesis, this evolution of the phase composition reflects very favorable conditions for the formation of the desired solid solution. On the basis of the low intensity of the  $\text{SrCrO}_4$  reflections, it can be asserted that, already in the samples resulting directly from the combustion synthesis, the projected substitution ( $\text{La}^{3+} \rightarrow \text{Sr}^{2+}$ ) was largely realized and the  $\text{La}_{0.7}\text{Sr}_{0.3}\text{CrO}_3$  phase was formed. When the temperature rises, the consumption of  $\text{SrCrO}_4$  continues due to its assimilation in the chromite phase and the oxidation number of the chromium from  $\text{SrCrO}_4$  reduces due to the release of oxygen surplus.

In fact, the dark brown color of the combustion-synthesized powders reflects the simultaneous presence of  $\text{Cr}^{3+}$  and  $\text{Cr}^{4+}$ , indicating that the partial substitution of  $\text{La}^{3+}$  by  $\text{Sr}^{2+}$  has already taken place to a certain extent. Considering the partial substitution of  $\text{La}^{3+}$  by  $\text{Sr}^{2+}$ , the oxidation of  $\text{Cr}^{3+}$  to  $\text{Cr}^{4+}$  is mandatory in order to preserve the electric neutrality of the crystalline lattice; for every  $\text{La}^{3+}$  cation substituted by a  $\text{Sr}^{2+}$  cation, one  $\text{Cr}^{3+}$  cation oxidizes to  $\text{Cr}^{4+}$ . After annealing, the color of the powders turns from dark brown to black,

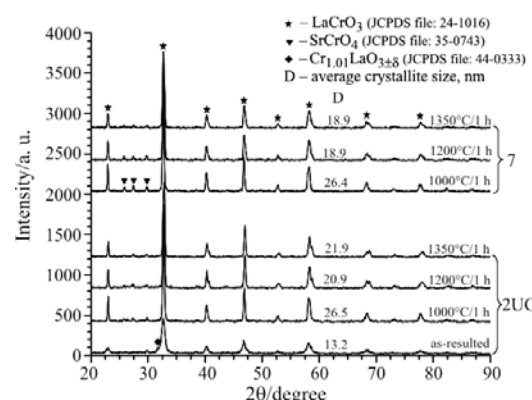


**Fig. 3** XRD patterns of the  $\text{La}_{0.7}\text{Sr}_{0.3}\text{CrO}_3$  powders prepared via combustion synthesis and organic precursors' method after annealing at different temperatures

suggesting that new amounts of  $\text{Cr}^{4+}$  have been produced as the result of incorporation of new amounts of  $\text{Sr}^{2+}$  from  $\text{SrCrO}_4$  into the perovskite solid solution.

Another important piece of evidence, which stands for this reaction mechanism, is represented by the evolution of the average crystallite size after annealing samples 7 and 2UG at various temperatures.

As seen in Fig. 3, after annealing at  $1200^\circ\text{C}$ , the resulting crystallites are smaller than the ones resulting after annealing at  $1000^\circ\text{C}$ . This apparent anomaly can be easily explained by considering the development of the solid-state reaction between  $\text{SrCrO}_4$  and the perovskite solid solution, which involves a certain degree of disorganization and reorganization of the crystalline lattice. It is very important to notice that this behavior does not appear in the case of samples with lower  $\text{Sr}^{2+}$  content ( $\text{La}_{0.9}\text{Sr}_{0.1}\text{CrO}_3$ ). At  $1350^\circ\text{C}$  in both synthesis methods – organic precursors and combustion synthesis – only small traces of  $\text{SrCrO}_4$  are detected, confirming the almost complete incorporation of  $\text{SrCrO}_4$  in the  $\text{LaCrO}_3$  structure yielding the  $\text{La}_{0.7}\text{Sr}_{0.3}\text{CrO}_3$  solid solution (Fig. 3).

In the case of stoichiometry with lower  $\text{Sr}^{2+}$  content ( $\text{La}_{0.9}\text{Sr}_{0.1}\text{CrO}_3$ ), the desired crystalline phase is obtained more easily. As seen in Table 2, the use of urea and glycine fuel mixture (Sample 5UG) allows the formation of pure nanocrystalline  $\text{La}_{0.9}\text{Sr}_{0.1}\text{CrO}_3$  directly from the combustion reaction, no additional annealing step being required (Fig. 4).

Unlike the combustion-synthesized  $\text{La}_{0.7}\text{Sr}_{0.3}\text{CrO}_3$  powders, which exhibit a dark brown color before annealing and a black one after annealing, the  $\text{La}_{0.9}\text{Sr}_{0.1}\text{CrO}_3$  powders exhibit a brown color, which does not change after annealing. The lighter color of  $\text{La}_{0.9}\text{Sr}_{0.1}\text{CrO}_3$  powders can be explained by the lower amount of doping  $\text{Sr}^{2+}$ , which involves a lower amount of  $\text{Cr}^{4+}$ .

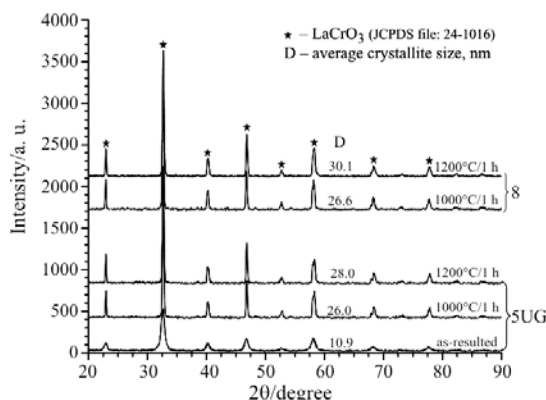


**Fig. 4** XRD patterns of the  $\text{La}_{0.9}\text{Sr}_{0.1}\text{CrO}_3$  prepared via combustion synthesis and organic precursors' method, after annealing at different temperatures

An important remark is that the brown color of the powder cannot be assigned to the presence of residual carbon because the losses on ignition are almost negligible (1.1%), but to the simultaneous presence of  $\text{Cr}^{3+}$  and  $\text{Cr}^{4+}$  due to the partial substitution of  $\text{La}^{3+}$  by  $\text{Sr}^{2+}$ . After annealing the sample at 1000°C with one hour soaking time, there are no modifications concerning the color of the powder or its phase composition, except for an improvement of the crystalline character evidenced by the increase in the average crystallite size (Fig. 4). All these observations point out that the partial substitution of  $\text{La}^{3+}$  by  $\text{Sr}^{2+}$ , which involves the partial oxidation of  $\text{Cr}^{3+}$  to  $\text{Cr}^{4+}$ , has already taken place during the combustion reaction.

On the other hand, in the case of the organic precursors' method, the formation of the perovskite phase requires annealing at 1000°C. As one could expect, after annealing at 1200°C, crystallites growth takes place, so that the average crystallites size is 30.1 nm (Fig. 4).

In case of samples with high  $\text{Sr}^{2+}$  content,  $\text{La}_{0.7}\text{Sr}_{0.3}\text{CrO}_3$ , the differences between the two synthesis methods are insignificant, considering the same annealing temperature required for the perovskite formation as a single phase. Nevertheless, it must be pointed out that in the case of combustion synthesis, the perovskite solid solution is the main crystalline phase, which results directly from the combustion reaction.

## Conclusions

- The two unconventional synthesis methods allow the formation of the perovskite solid solutions,  $\text{La}_{1-x}\text{Sr}_x\text{CrO}_3$  ( $x=0.1$  and 0.3), at lower temperatures than in the case of the ceramic method, based on annealing mechanical mixtures of oxides and/or salts.

- For lower  $\text{Sr}^{2+}$  content,  $\text{La}_{0.9}\text{Sr}_{0.1}\text{CrO}_3$ , the perovskite phase results directly from the combustion reaction, without the necessity for additional thermal treatments. Using the organic precursors' method, the formation of  $\text{La}_{0.9}\text{Sr}_{0.1}\text{CrO}_3$  requires annealing at 1000°C.
- The average crystallite size of the combustion-synthesized powders is directly influenced by the nature of the fuel.
- As the  $\text{Sr}^{2+}$  content increases, its inclusion into the perovskite phase takes place more difficult and a higher annealing temperature is required. Although in the case of combustion synthesis the resulting powder already contains  $\text{La}_{0.7}\text{Sr}_{0.3}\text{CrO}_3$  as the main crystalline phase, some of the  $\text{Sr}^{2+}$  content is immobilized in  $\text{SrCrO}_4$ . The inclusion of  $\text{SrCrO}_4$  into the desired crystalline phase requires annealing at 1350°C. From this point of view similar results were obtained using the organic precursors' method.

## References

- O. Yamamoto, Electrochim. Acta, 45 (2004) 1423.
- E. S. M. Seo, W. K. Yoshito, V. Ussui, D. R. R Lazar, S. R. H. M. Castanho and J. O. A. Paschoal, Mater. Res., 7 (2004) 215.
- J. W. Fergus, Solid State Ionics, 171 (2004) 1.
- N. Sakai, H. Yokokawa, T. Horita and K. Yamaji, Int. J. Appl. Ceram. Tech., 1 (2004) 23.
- P. H. Larsen, P. V. Hendriksen and M. Mogensen, J. Therm. Anal. Cal., 49 (1997) 1263.
- M. R. Guire, S. E. Dorris, R. B. Poepel, S. Morissette and U. Balachandran, J. Mater. Sci., 8 (1993) 2327.
- S. Bilger, G. Blaß and R. Förthmann, J. Eur. Ceram. Soc., 17 (1997) 1027.
- D. Berger, V. Fruth and I. Jitaru, Mater. Lett., 58 (2004) 2418.
- D. Berger, I. Jitaru, N. Stanica, R. Perego and J. Schoonman, J. Mater. Synth. Process., 9 (2001) 137.
- L. P. Rivas-Vazquez, J. C. Rendon-Angeles, J. L. Rodriguez-Galicia, K. Zhu and K. Yanagisawa, Solid State Ionics, 172 (2004) 389.
- L. P. Rivas-Vazquez, J. C. Rendon-Angeles, J. L. Rodriguez-Galicia, C. A. Gutierrez-Chavarria, K. J. Zhu and K. Yanagisawa, J. Eur. Ceram. Soc., 26 (2006) 81.
- T. Lone-Wen and A. A. Lessing, J. Mater. Res., 7 (1992) 511.
- Y. S. Malghe and S. R. Dharwadkar, J. Therm. Anal. Cal., 91 (2008) 915.
- S. Biamino and C. Badini, J. Eur. Ceram. Soc., 24 (2004) 3021.
- E. P. Marinho, A. G. Souza, D. S. de Melo, I. M. G. Santos, D. M. A. Melo and W. J. da Silva, J. Therm. Anal. Cal., 87 (2007) 801.
- A. S. Mukasyan, C. Costello, K. P. Sherlock, D. Lafarga and A. Varma, Sep. Purif. Technol., 25 (2001) 117.
- D. Kishori, A. Mukasyan and A. Varma, J. Am. Ceram. Soc., 86 (2003) 1149.

- 18 Y. Yong-Jie, W. Ting-Lian, T. Hengyong, W. Da-Qian and Y. Jianhua, Solid State Ionics, 135 (2000) 475.
- 19 G. Zhu, X. Fang, C. Xia and X. Liu, Ceram. Int., 31 (2005) 115.
- 20 Z. Zhong, Solid State Ionics, 177 (2006) 757.
- 21 K. Zupan, D. Kolar and M. Marinšek, J. Power Sources, 86 (2000) 417.
- 22 K. Zupan, S. Pejovnik and J. Maček, Acta Chim. Slov., 48 (2001) 137.
- 23 I. Lazău, C. Păcurariu and R. I. Lazău, Interceram, 51 (2002) 266.
- 24 C. Păcurariu, I. Lazău, Z. Ecsedi, R. Lazău, P. Barvinschi and G. Mărginean, J. Eur. Ceram. Soc., 27 (2007) 707.
- 25 R. Ianoş, I. Lazău, C. Păcurariu and P. Barvinschi, Eur. J. Inorg. Chem., (2008) 925.
- 26 R. Ianoş, I. Lazău, C. Păcurariu and P. Barvinschi, Eur. J. Inorg. Chem., (2008) 931.
- 27 A. Ianculescu, A. Brăileanu, I. Pasuk and M. Zaharescu, J. Therm. Anal. Cal., 66 (2001) 501.

---

DOI: 10.1007/s10973-008-9104-1